THE JOURNAL OF BIOLOGICAL CHEMISTRY VOL. 290, NO. 37, pp. 22724–22733, September 11, 2015

Kv4.2 and Accessory Dipeptidyl Peptidase-like Protein 10 (DPP10) Subunit Preferentially Form a 4:2 (Kv4.2:DPP10) Channel Complex*[S]

Received for publication, February 19, 2015, and in revised form, July 21, 2015 Published, JBC Papers in Press, July 24, 2015, DOI 10.1074/jbc.M115.646794

Masahiro Kitazawa, Yoshihiro Kubo[1], and Koichi Nakajo[2]

From the Division of Biophysics and Neurobiology, Department of Molecular Physiology, National Institute for Physiological Sciences, Okazaki, Aichi 444-8585, Japan and the Department of Physiological Sciences, Graduate University for Advanced Studies (SOKENDAI), Hayama, Kanagawa 240-0155, Japan

Background: Kv4-DPP forms a complex of unknown stoichiometry.
Results: Kv4.2-DPP10 current properties and stoichiometry are altered depending on their relative expression levels.
Conclusion: The stoichiometry of Kv4.2-DPP10 is variable with a preference for the 4:2 configuration.
Significance: Kv4-DPP stoichiometry may provide important information for the treatment of some psychiatric diseases.

Kv4 is a member of the voltage-gated K^+ channel family and forms a complex with various accessory subunits. Dipeptidyl aminopeptidase-like protein (DPP) is one of the auxiliary subunits for the Kv4 channel. Although DPP has been well characterized and is known to increase the current amplitude and accelerate the inactivation and recovery from inactivation of Kv4 current, it remains to be determined how many DPPs bind to one Kv4 channel. To examine whether the expression level of DPP changes the biophysical properties of Kv4, we expressed Kv4.2 and DPP10 in different ratios in *Xenopus* oocytes and analyzed the currents under two-electrode voltage clamp. The current amplitude and the speed of recovery from inactivation of Kv4.2 changed depending on the co-expression level of DPP10. This raised the possibility that the stoichiometry of the Kv4.2-DPP10 complex is variable and affects the biophysical properties of Kv4.2. We next determined the stoichiometry of DPP10 alone by subunit counting using single-molecule imaging. Approximately 70% of the DPP10 formed dimers in the plasma membrane, and the rest existed as monomers in the absence of Kv4.2. We next determined the stoichiometry of the Kv4.2-DPP10 complex; Kv4.2-mCherry and mEGFP-DPP10 were co-expressed in different ratios and the stoichiometries of Kv4.2-DPP10 complexes were evaluated by the subunit counting method. The stoichiometry of the Kv4.2-DPP10 complex was variable depending on the relative expression level of each subunit, with a preference for 4:2 stoichiometry. This preference may come from the bulky dimeric structure of the extracellular domain of DPP10.

Kv4, a member of the voltage-gated K^+ channel (Kv)[3] family, is expressed in neurons and cardiac myocytes. In neurons, Kv4 contributes to the somatodendritic subthreshold A-type current (I_{SA}), which is involved in the control of repetitive firing and the attenuation of the back-propagation of action potentials (1–5). In cardiac ventricular myocytes, Kv4 generates the transient outward K^+ current (I_{to}), which plays an important role in the early phase of cardiac action potential repolarization (6–14). Kv4 forms multimolecular complexes with various subunits under physiological conditions (14–20). Dipeptidyl aminopeptidase-like protein (DPP) is one of the accessory subunits for Kv4 and was originally identified as a 115-kDa protein (21–24). DPPs belong to the prolyl oligopeptidase subfamily of the serine protease family and contain a well known catalytic triad (Ser/His/Asp). However, DPP6 (also known as DPPX) and DPP10 (DPPY) lack the catalytic serine (it is substituted to aspartic acid in DPP6 or glycine in DPP10) and hence lack catalytic activity (18, 25–27). The common molecular structure of the DPP family comprises a short N-terminal region, a single-transmembrane region, and a large extracellular C-terminal region including a glycosylation domain, a cysteine-rich domain, and an aminopeptidyl peptidase-like domain (21).

DPP6 is expressed in many regions of the brain including hippocampal CA1 neurons, where it controls the A-current (Kv4) expression level and even dendritic morphogenesis by interacting with fibronectin in the extracellular matrix (28, 29). DPP6 has been implicated in neuropsychiatric pathologies including autism spectrum disorders (30, 31), mental retardation (32), and amyotrophic lateral sclerosis (33, 34). DPP10 is also broadly expressed in the brain including the hippocampus, neocortex, cerebellum, and main olfactory bulb, where Kv4-KChIP-DPP form a ternary complex (35). DPP10 is also implicated in neuropsychiatric diseases such as autism (30, 36) and Alzheimer disease (37). Therefore, the Kv4-KChIP-DPP com-

* This study was supported by a grant-in-aid for scientific research (KAKENHI) from the Japan Society for the Promotion of Science (to K. N. and Y. K.). The authors declare that they have no conflicts of interest with the contents of this article.
[S] This article contains supplemental Movies 1–3.
[1] To whom correspondence may be addressed: Div. of Biophysics and Neurobiology, Dept. of Molecular Physiology, Natl. Inst. for Physiological Sciences, Okazaki, Aichi 444-8585, Japan. Tel.: 81-564-55-7831; Fax: 81-564-55-7834; E-mail: ykubo@nips.ac.jp.
[2] To whom correspondence may be addressed: Dept. of Physiology, Osaka Medical College, Takatsuki, Osaka 569-8686, Japan. Tel.: 81-72-684-7283; Fax: 81-72-684-6521; E-mail: knakajo@art.osaka-med.ac.jp.

[3] The abbreviations used are: Kv, voltage-gated K^+ channel; DPP, dipeptidyl aminopeptidase-like protein; KChIP, K^+ channel-interacting protein; TIRF, total internal reflection fluorescence; mEGFP, monomeric enhanced green fluorescent protein; mCherry, monomeric cherry red fluorescent protein; KD, Kv4.2-DPP6 construct; KKD, Kv4.2-Kv4.2-DPP6 construct.

plex could be a good target for therapeutic approaches to these diseases, although a better understanding of the complex composition and formation would be required.

DPP increases the current amplitude of Kv4 both by increasing the single-channel conductance and by facilitating the trafficking of Kv4 protein from the endoplasmic reticulum to the plasma membrane (38–41). DPP also accelerates both the inactivation and the recovery from inactivation of Kv4, although the underlying mechanism has not been fully determined (42–46). The region from the N terminus to the start of the transmembrane domain of DPP10 plays an important role in binding to the S1-S2 segments of Kv4 in complex formation (47). However, it remains uncertain how many DPP subunits can bind to a tetrameric Kv4 channel. Although there is no available crystal structure for the Kv4-DPP complex, a crystal structure of the extracellular domains of DPP6/10 has been determined, and it is suggested that DPP6 and DPP10 exist as a dimer in the plasma membrane (26, 48). This implies the possibility that Kv4 and DPP preferentially form a 4:2 (Kv4:DPP) channel. On the other hand, a previous experiment using tandem repeat constructs suggests that the Kv4.2 channel requires four DPP6 subunits to be fully modulated (49).

We reported previously that the stoichiometry of Kv4 and another accessory subunit, KChIP, is variable and concluded that up to four KChIP molecules can bind to a single Kv4 tetramer (4:4 stoichiometry) (50). The stoichiometry of Kv4-KChIP is dependent on the relative expression levels of KChIP and Kv4 with no preferred stoichiometry (50).

In the present study, we aimed to determine the stoichiometry of Kv4 and DPP10. We first examined how the expression level of DPP10 affects the electrophysiological properties of Kv4.2 and observed that the current amplitude and the recovery from inactivation changed depending on the expression level of DPP10. Next, we confirmed the dimeric structure of DPP10 alone in the plasma membrane by subunit counting using single-molecule imaging under total internal reflection fluorescence (TIRF) microscopy. Interestingly, ~70% of DPP10 on the plasma membrane existed as dimers and the rest existed as monomers. Finally, we determined the stoichiometry of the Kv4.2-DPP10 complex. The stoichiometry of the Kv4.2-DPP10 complex was again variable and dependent on the expression level of DPP10 as is the case for the Kv4-KChIP complex (50). However, in contrast, Kv4.2-DPP10 showed a clear preference for the 4:2 stoichiometry, probably because of the large dimeric extracellular domain.

Experimental Procedures

Molecular Biology—Human Kv4.2 (DNA Data Bank of Japan (DDBJ) accession number AB028967) and human DPP10d (DDBJ accession number AB040925) (44, 45) were provided by Kazusa DNA Research Institute and were subcloned into the pGEMHE expression vector. mEGFP and mCherry with a flexible linker were kindly provided by Dr. M. Ulbrich (University of Freiburg) (51, 52). mEGFP tagged Kv4.2 (Kv4.2-mEGFP) was constructed as described previously (50). For mEGFP-DPP10, a XhoI site was added to the N terminus of DPP10, and a cleavage was made at the unique BstXI site in DPP10 (XhoI-DPP10-BstXI). mEGFP with a flexible GGS linker on the C terminus was cleaved at the unique XhoI site in the linker, and cleavage was made at the unique KpnI site in the pGEMHE vector (KpnI-mEGFP-linker-XhoI). The two fragments were ligated at the XhoI sites and inserted into the KpnI and BstXI sites in the DPP10-pGEMHE construct. A C-terminal truncated version of mEGFP-DPP10 (mEGFP-DPP10-D-Extra) was made by PCR as described previously (41). To construct Kv4.2-mCherry, a BglII site was introduced into the N terminus of mCherry with a flexible GGS linker (BglII-mCherry). mEGFP in Kv4.2-mEGFP was then replaced with mCherry by using the BglII site. All constructs were confirmed by DNA sequencing. cRNA was transcribed from the linearized plasmid cDNA using a T7 mMessage mMachine kit (Ambion).

Preparation of Xenopus Oocytes—Oocytes were surgically obtained from *Xenopus laevis* anesthetized in water containing 0.15% tricaine for 30 min. *Xenopus* frogs were allowed to recover from anesthesia before being returned to the tank. To remove the follicular cell layer, oocytes were treated with collagenase for 6–7 h at room temperature. Defolliculated oocytes of similar size at stage V or VI were microinjected with 50 nl of cRNA solution and incubated for 1–3 days at 17 °C in frog Ringer solution containing (in mM): 88 NaCl, 1 KCl, 2.4 $NaHCO_3$, 0.3 $Ca(NO_3)_2$, 0.41 $CaCl_2$, and 0.82 $MgSO_4$, pH 7.6, with 0.1% penicillin-streptomycin solution (Sigma-Aldrich). All experiments were approved by the Animal Care Committee of the National Institute for Physiological Sciences (Japan) and were performed following the institutional guidelines.

Two-electrode Voltage Clamp—One to 3 days after cRNA injection, ionic currents were recorded under two-electrode voltage clamp with an OC-725C amplifier (Warner Instruments) at room temperature. The bath chamber was perfused with ND-96 containing (in mM): 96 NaCl, 2 KCl, 1.8 $CaCl_2$, 1 $MgCl_2$, and 5 HEPES, pH 7.2. The microelectrodes were drawn from borosilicate glass capillaries (World Precision Instruments) to a resistance of 0.2–0.5 megohm and filled with 3 M potassium acetate and 10 mM KCl, pH 7.2. Holding potential was −80 mV or −100 mV. Voltage clamp protocols and data acquisition were performed using a digital converter (Digidata 1440) and pCLAMP 10.3 software (Molecular Devices).

Subunit Counting by Single-molecule Imaging—Twelve to 20 h after cRNA injection, to remove the extracellular matrix the oocytes were treated with 1 unit/ml neuraminidase (Sigma-Aldrich) and 1 mg/ml hyaluronidase (Sigma-Aldrich) for 15 min at 12 °C (52). To remove the vitelline membrane, oocytes were put into 2× frog Ringer solution, which makes them shrink osmotically. The vitelline membrane was then manually removed with forceps. The oocytes were put on a high refractive index coverslip ($n = 1.78$) (Olympus) and observed through an objective lens (Olympus ×100, N.A. 1.65) mounted on an inverted microscope (Olympus IX71). Movies of 400 frames (20 Hz, 20 s) were recorded with an iXon3 EMCCD camera (Andor) and Solis software (Andor). ND-96 was used as the extracellular solution. mEGFP was excited with a cyan 488-nm solid laser (Spectra-Physics), and mCherry was excited with an orange 588-nm solid laser (Coherent Inc.). The density of the ion channels was kept low enough (~1 spot/μm^2) to minimize the probability of two spots overlapping within a diffraction-limited spot (52, 53). A 25.6 × 25.6-μm^2 area was illuminated,

and the fluorescence intensity of each spot was measured off-line from the recorded movie. Stable spots throughout the recording were selected manually to analyze the bleaching steps and the overlap of green and red spots.

Data Analysis for Electrophysiology—pCLAMP 10.3 (Molecular Devices) and IGOR Pro software (WaveMetrics, Inc.) were utilized for the ionic current analyses. All current traces were analyzed without leak subtraction.

The kinetics of the recovery from inactivation was fitted with a single exponential function,

$$I = I_{peak}(1 - e^{-t/\tau_{rec}}) \quad \text{(Eq. 1)}$$

where I_{peak} is the average of peak current amplitudes at prepulse and τ_{rec} is the recovery time constant at −100 mV.

Data Analysis for Subunit Counting—The number of subunits in the optical spots was analyzed based on the distribution histogram of the bleaching steps. The obtained histograms were fitted with a binomial distribution, $P(X = a)$,

$$P(X = a) = A_n C_a p^a (1 - p)^{n-a} \quad \text{(Eq. 2)}$$

where A is the total number of spots, ${}_nC_a$ is the number of combinations of choosing a from among n, n is the number of bound subunits, a is the number of observed bleaching steps, and p is the fluorescence probability of mEGFP.

Statistical Analyses—All data are presented as the mean ± S.E., and n represents the number of samples. Statistical differences were evaluated using the Tukey-Kramer test. Values of $p < 0.05$ were considered significant, and *** indicates $p < 0.001$.

Results

DPP10 Changes Kv4.2 Properties in an Expression Level-dependent Manner—DPP10 is an accessory subunit for Kv4 that is known to increase the current amplitude of Kv4.2 and to accelerate the inactivation and recovery from inactivation of Kv4.2 (38, 42, 54). In our previous report, we demonstrated that the biophysical properties of Kv4.2 change with increasing expression level of KChIP4 (50). Here, we first investigated whether the biophysical properties of Kv4.2 were also variable and dependent on the expression level of DPP10 as in the case of KChIP4. 2.5 ng of Kv4.2 cRNA was injected with various amounts of DPP10 cRNA (0, 0.025, 0.25, and 2.5 ng) into *Xenopus* oocytes, and the currents were recorded under two-electrode voltage clamp at 1 to 3 days after the injection. Kv4.2 current was evoked by depolarizing pulses from −100 to +50 mV (Fig. 1*A*). The current amplitudes were not significantly changed by up to 0.25 ng of DPP10 cRNA but were changed significantly between 0.25 ng (3.2 ± 0.4 μA, $n = 19$) and 2.5 ng (8.6 ± 1.2 μA, $n = 10$; $p < 0.001$) (Fig. 1*B*). On the other hand, the normalized *I*-V relationships were not significantly different among groups (Fig. 1*C*).

Another prominent change induced by DPP10 co-expression was in the kinetics of the recovery from inactivation. To evaluate the recovery from inactivation, a +40-mV depolarizing prepulse was applied for 500 ms to fully inactivate the current, and a second +40-mV test pulse was subsequently applied after hyperpolarizing at −100 mV for 10–490 ms to measure the recovery (Fig. 2*A*). The time course of the recovery from inactivation was best fitted with a single exponential function (Fig. 2*B*). The time constant was decreased from 145.9 ± 2.7 ms (Kv4.2 (2.5 ng) with DPP10 (0.025 ng), $n = 7$) to 69.3 ± 3.2 ms (Kv4.2 (2.5 ng) with DPP10 (2.5 ng), $n = 8$; $p < 0.001$), suggesting that the recovery from inactivation of Kv4.2 accelerated when more than 0.25 ng of DPP10 cRNA was injected with Kv4.2 cRNA (Fig. 2*C*).

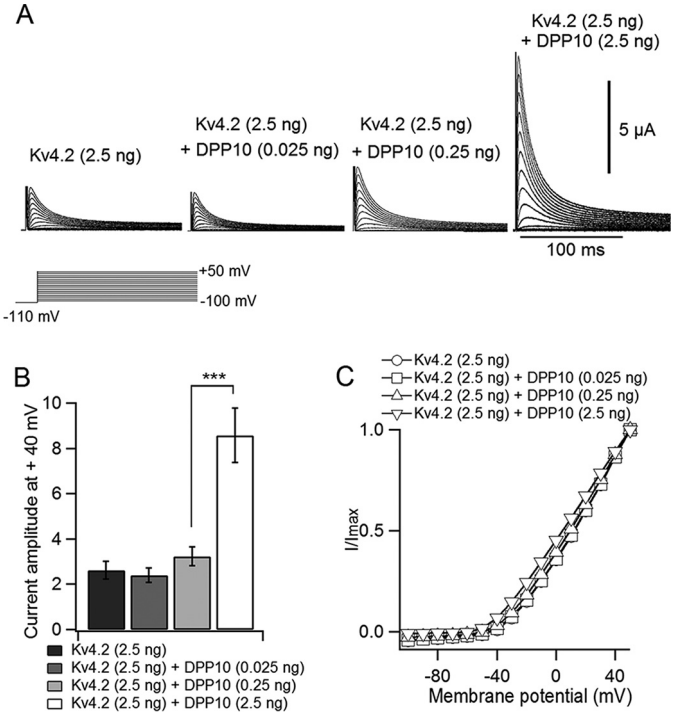

FIGURE 1. **The expression level of DPP10 affects the current amplitude of Kv4.2.** *A*, representative current traces of Kv4.2 (2.5 ng) with DPP10 (0, 0.025, 0.25, and 2.5 ng) are shown. The holding potential was −80 mV. After 500 ms of hyperpolarization at −110 mV to remove inactivation, currents were elicited by depolarizing the voltage steps for 1 s between −100 mV and +50 mV in 10-mV increments. Current traces of the first 150 ms are shown. *B*, current amplitudes of Kv4.2 with various expression levels of DPP10 are compared ($n = 10$–19). The *error bars* represent S.E. ***, indicates $p < 0.001$. *C*, *I*-V relationships of Kv4.2 without DPP10 (*open circles*) and with DPP10 (0.025 ng, *open squares*; 0.25 ng, *open triangles*; and 2.5 ng, *open inverted triangles*). Peak current amplitudes at each membrane potential taken from *A* are normalized by the peak current amplitude at +50 mV ($n = 10$–19).

Taking these results together, the current amplitude and the recovery from inactivation were changed depending on the expression level of DPP10. This raised the possibility that the stoichiometry of the Kv4.2-DPP10 complex might be variable and dependent on the relative expression level of each subunit as we had observed previously for the Kv4.2-KChIP4 complex (50).

Approximately 70% of the DPP10 on the Membrane Exists as Dimers—The determination of stoichiometry had not been an easy task when using a classical biochemical method. However, the recent development of single-molecule imaging enabled us to count the number of molecules directly (52, 53, 55). The idea of this method is that one can count the number of subunits in a single-membrane protein complex (*e.g.* ion channel tetramer) by counting irreversible bleaching steps from a fluorescence-tagged protein (*e.g.* GFP-tagged subunit): one step means a single bleaching event of GFP, indicating the existence of single

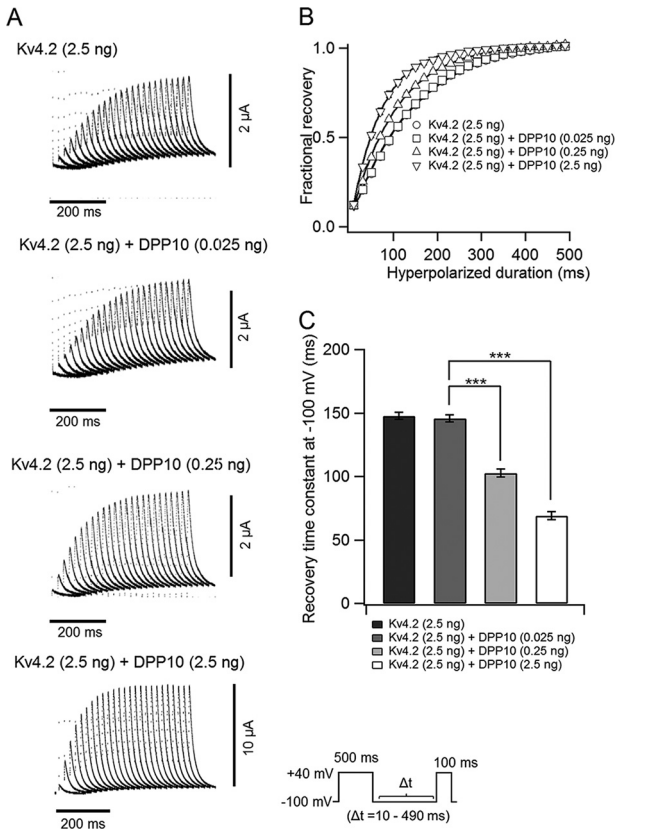

FIGURE 2. **The recovery from inactivation of Kv4.2 is gradually accelerated with increasing expression level of DPP10.** *A*, representative current traces showing the recovery from inactivation. Various amounts of DPP10 cRNA (0, 0.025, 0.25, and 2.5 ng) were co-injected with 2.5 ng of Kv4.2 cRNA. The currents were elicited by a two-pulse protocol (*inset*). The currents evoked by the prepulse was omitted, and only the currents evoked by the second test pulses are presented. *B*, kinetics of the recovery from inactivation of Kv4.2 with various expression levels of DPP10 (0 ng, *open circles*; 0.025 ng, *open squares*; 0.25 ng, *open triangles*; 2.5 ng, *open inverted triangles*) ($n = 7–9$). Peak current amplitudes during the second +40-mV step were normalized by the average of the peak current amplitude during the +40-mV prepulse. *C*, time constants of the recovery from inactivation of Kv4.2 with different DPP10 expression levels. The time constants are obtained by fitting the curves taken from *B* with a single exponential function. *Error bars* are S.E. ***, indicates $p < 0.001$.

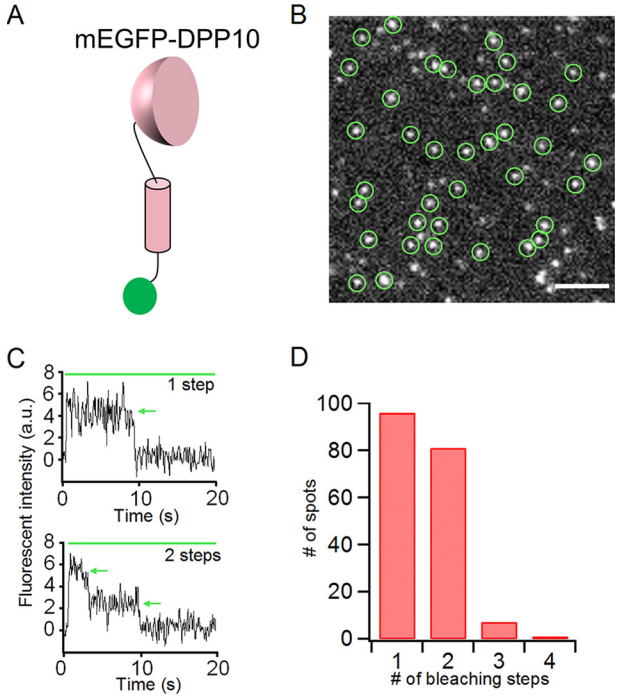

FIGURE 3. **Approximately 70% of DPP10 exists as dimers.** *A*, schematic illustration of mEGFP-DPP10. mEGFP was fused to the intracellular N terminus of DPP10. *B*, a single frame from a TIRF movie from a *Xenopus* oocyte expressing mEGFP-DPP10. The *green circles* indicate the fluorescent spots of mEGFP-DPP10. *Scale bar* = 2 μm. *C*, representative traces of fluorescence intensity taken from the fluorescent spots in *B*. The *green bars* show the time of illumination with a 488-nm laser. The *green arrows* indicate the bleaching steps. *D*, a histogram of the observed distribution of the number of bleaching steps.

subunit. It is an especially powerful method for examining stoichiometry because each individual macromolecule complex can be evaluated (counted) (50, 51, 56, 57). Before determining the stoichiometry of the Kv4.2-DPP10 complex, we first determined the stoichiometry of DPP10 alone.

DPP6 is a member of the dipeptidyl aminopeptidase-like protein family and is also known as an accessory subunit for Kv4 (29, 58, 59). The crystal structure of the extracellular domain shows that DPP6 forms a dimeric structure (26). The recently published crystal structure of the extracellular domain of DPP10 shows a similar dimeric structure (48). To examine whether the full-length DPP10 actually exists as a dimer in the membrane, we constructed mEGFP-tagged DPP10 (mEGFP-DPP10) in which mEGFP was fused to the intracellular N terminus of DPP10 (Fig. 3*A*). mEGFP-DPP10 alone was expressed in *Xenopus* oocytes, and the fluorescent spots were observed under TIRF illumination (Fig. 3*B* and supplemental Movie 1). We counted the bleaching steps from 185 spots in total, and the numbers of spots for each bleaching step were plotted as a histogram (Fig. 3, *C* and *D*). Most of the spots showed one or two bleaching steps with a few exceptions of three or four bleaching steps (probably due to an occasional overlapping of two fluorescent spots (53)), suggesting that DPP10 exists as dimers, as expected from the DPP6/10 structures, and possibly also as monomers (Fig. 3, *C* and *D*). We then estimated the proportion of monomers, if present, and dimers based on a binomial distribution, with a variable fluorescence probability p (Table 1). According to some previous reports, the probability that mEGFP is fluorescent is around 0.7–0.8 (50–52). If that was also the case here, 65–81% of the spots on the membrane would be dimers and the rest would exist as monomers (Table. 1).

A 4:2 Stoichiometry Is Preferred in the Kv4.2-DPP10 Complex—Next we determined the stoichiometry of Kv4.2 and DPP10. To identify mEGFP-DPP10 co-assembled with Kv4.2, Kv4.2 was tagged with the red fluorescent protein mCherry (Kv4.2-mCherry) (Fig. 4*A*). We first confirmed that Kv4.2-mCherry (2.5 ng) and mEGFP-DPP10 were functional. Kv4.2-mCherry (2.5 ng) with mEGFP-DPP10 (2.5 ng) showed fast inactivating currents similar to those of wild-type Kv4.2 (2.5 ng) with wild-type DPP10 (2.5 ng) (Fig. 4*B*). To confirm the co-assembly of Kv4.2-mCherry and mEGFP-DPP10, mCherry was first excited with a 588-nm laser (Fig. 4*C*, *left*), and mEGFP was subsequently excited with a 488-nm laser (Fig. 4*C*, *middle*, and supplemental Movie 2). The mCherry and mEGFP frames from the obtained movie were superimposed (Fig. 4*C*, *right*); the *yellow spots* indicate co-assembly of Kv4.2-mCherry and mEGFP-DPP10. To examine the idea of variable stoichiometry, Kv4.2-

TABLE 1

Calculated proportion of dimers and monomers of DPP10 on the plasma membrane

The proportions of dimeric and monomeric DPP10 are based on the distribution shown in Fig. 3*D*. The value of fluorescence probability of mEGFP (*p*) was changed between 0.63 and 1.

p	Dimer	Monomer
1	0.46	0.54
0.9	0.54	0.46
0.8	0.65	0.35
0.7	0.81	0.19
0.63	0.99	0.01

mCherry and mEGFP-DPP10 were co-expressed in *Xenopus* oocytes with various cRNA ratios (100:1 (1:0.01 ng), 10:1 (1:0.1 ng), and 1:1 (0.1:0.1 ng)), and the bleaching steps from each mEGFP fluorescent spot were counted (Fig. 4*D*). Throughout the three different expression levels, the two bleaching step spots were consistently predominant, although the three- and four-step bleaching spots gradually increased with increasing DPP10 expression (Fig. 4*E*). The result suggests that the stoichiometry of the Kv4.2-DPP10 complex is variable depending on the expression level of DPP10 and preferentially forms the 4:2 (Kv4.2:DPP10) complex.

Co-expression of KChIP4 Does Not Significantly Change the Stoichiometry of the Kv4.2-DPP10 Complex—It is known that Kv4, DPP, and KChIP form a ternary complex in neurons (35, 60, 61). To examine whether the co-expression of KChIP4 affects the stoichiometry of the Kv4.2-DPP10 complex, Kv4.2-mCherry, mEGFP-DPP10, and KChIP4 were all co-expressed (Fig. 5*A*). Before analyzing the stoichiometry of the Kv4.2-DPP10 complex, we first confirmed that the co-expression of KChIP4 modulated the ionic current of the Kv4.2-mCherry/mEGFP-DPP10 complex as expected. The inactivation of the Kv4.2-mCherry/mEGFP-DPP10 complex in the presence of KChIP4 (Fig. 5*B*, *bottom*) was apparently slower compared with the case in the absence of KChIP4 (Fig. 4*B*, *bottom*) and showed similar kinetics to those of wild-type Kv4.2, DPP10, and KChIP4 (Fig. 5*B*, *top*). The stoichiometry of the Kv4.2-DPP10 complex with various ratios of Kv4.2, DPP10, and KChIP4 (Kv4.2-mCherry:mEGFP-DPP10:KChIP4 = 100:1:100 (5:0.05:5 ng), 10:1:10 (5:0.5:5 ng), and 1:1:1 (1:1:1 ng)) was examined by subunit counting. In all three cases, the two-step bleaching spots were predominant and the three- and four-step bleaching spots were increased along with increasing mEGFP-DPP10 expression (Fig. 5*C*). Compared with the stoichiometry of the Kv4.2-DPP10 complex in the absence of KChIP4 (Fig. 4*E*), no notable stoichiometry changes were observed in the presence of KChIP4. As we had shown previously that the stoichiometry of Kv4.2/KChIP4 is independent of DPP10 (50), the stoichiometry of the Kv4.2-DPP10 complex was now shown to be independent of KChIP4 expression as well.

The Extracellular Domain of DPP10 May Prevent the Binding of Third and Fourth DPP10 Subunits to the 4:2 Channel—The extracellular domain of DPP6/10 forms a dimeric structure according to the crystal structure (26, 48) and our subunit counting experiment (Fig. 3). Because the extracellular domain is large (residues 50–789) and bulky, we predicted that a deletion of the extracellular domain might change the preference of the 4:2 stoichiometry in the Kv4.2-DPP10 complex. Lin *et al.* (41) recently made the deletion mutant of DPP6 (DPP6-D-Extra), which lacks the entire C-terminal extracellular domain. Interestingly, DPP6-D-Extra is very well expressed on the cell surface of HEK293 cells and accelerates the recovery from inactivation, yet it fails to increase the current amplitude (41). To examine whether the extracellular domain has an influence on the stoichiometry of Kv4.2-DPP10, we made a similar C-terminal deletion mutant, DPP10-D-Extra, which lacks the entire extracellular domain (residues 50–789) (Fig. 6*A*). First, we injected cRNA of mEGFP-DPP10-D-Extra (2 ng) alone and observed the expression in *Xenopus* oocytes. This was well expressed on the cell surface, in agreement with Lin *et al.* (41). Most of the fluorescent spots were mobile (supplemental Movie 3), in sharp contrast to mEGFP-DPP10 with the extracellular domain, which mostly stayed in the same place (supplemental Movie 1). Because DPP6 interacts with fibronectin in the extracellular matrix (28), DPP10 may also bind to the extracellular matrix via the extracellular domain and remain fixed.

Kv4.2 (10 ng of cRNA) and mEGFP-DPP10-D-Extra (0.1 ng) were then co-expressed in *Xenopus* oocytes. Probably because DPP10-D-Extra mutants were mobile, fewer co-localized spots were found (Fig. 6*B*, *white arrowheads*) than with the combination of Kv4.2 and DPP10 (Fig. 4*C*). Nevertheless, we were able to collect 158 countable spots. Even at this cRNA ratio (100:1), we observed a substantial number of three- and four-step bleaching spots (Fig. 6*C*). The distribution of bleaching steps looked more similar to the distribution of the 1:1 cRNA ratio than that of the 100:1 ratio in Kv4.2-DPP10 (Fig. 4*E*). This result suggests that the dimeric extracellular domains of DPP10 probably prevent binding of the third and fourth DPP10 subunits to Kv4.2. This is the reason that the 4:2 stoichiometry is preferred in the Kv4.2 and full-length DPP10 complex.

Discussion

In this study, we obtained three findings as follows. First, we showed that the electrophysiological properties of Kv4.2 are affected by the expression level of DPP10 (Figs. 1 and 2). Second, ~70% of DPP10 on the membrane exists as dimers, and the rest exists as monomers (Fig. 3). Third, the stoichiometry of the Kv4.2-DPP10 complex changes depending on the expression level of each subunit, with a tendency to form a 4:2 (Kv4.2:DPP10) channel probably because of the dimeric nature of the extracellular domain (Figs. 4, 6, and 7*A*). These observations can be explained in accordance with the current view of the Kv4.2 multimolecular complex as follows.

Variable Stoichiometry and Function of the Kv4.2-DPP10 Complex—In our electrophysiological experiments, we observed that the current amplitude of Kv4.2 increased with the expression of DPP10 (2.5 ng) (Fig. 1). There are two reported mechanisms by which DPP6/10 boosts the Kv4 current. DPP6 (and probably DPP10) increases the single-channel conductance of Kv4.2 (39). It has also been demonstrated that co-expression of DPP6/10 facilitates the surface expression of Kv4.2 through an effect on the endoplasmic reticulum (62). Therefore, the augmentation of the Kv4.2 current amplitude observed in Fig. 1 is caused by both or either an increase in the single-channel conductance and/or the number of Kv4.2 channels expressed in the plasma membrane. We also observed that

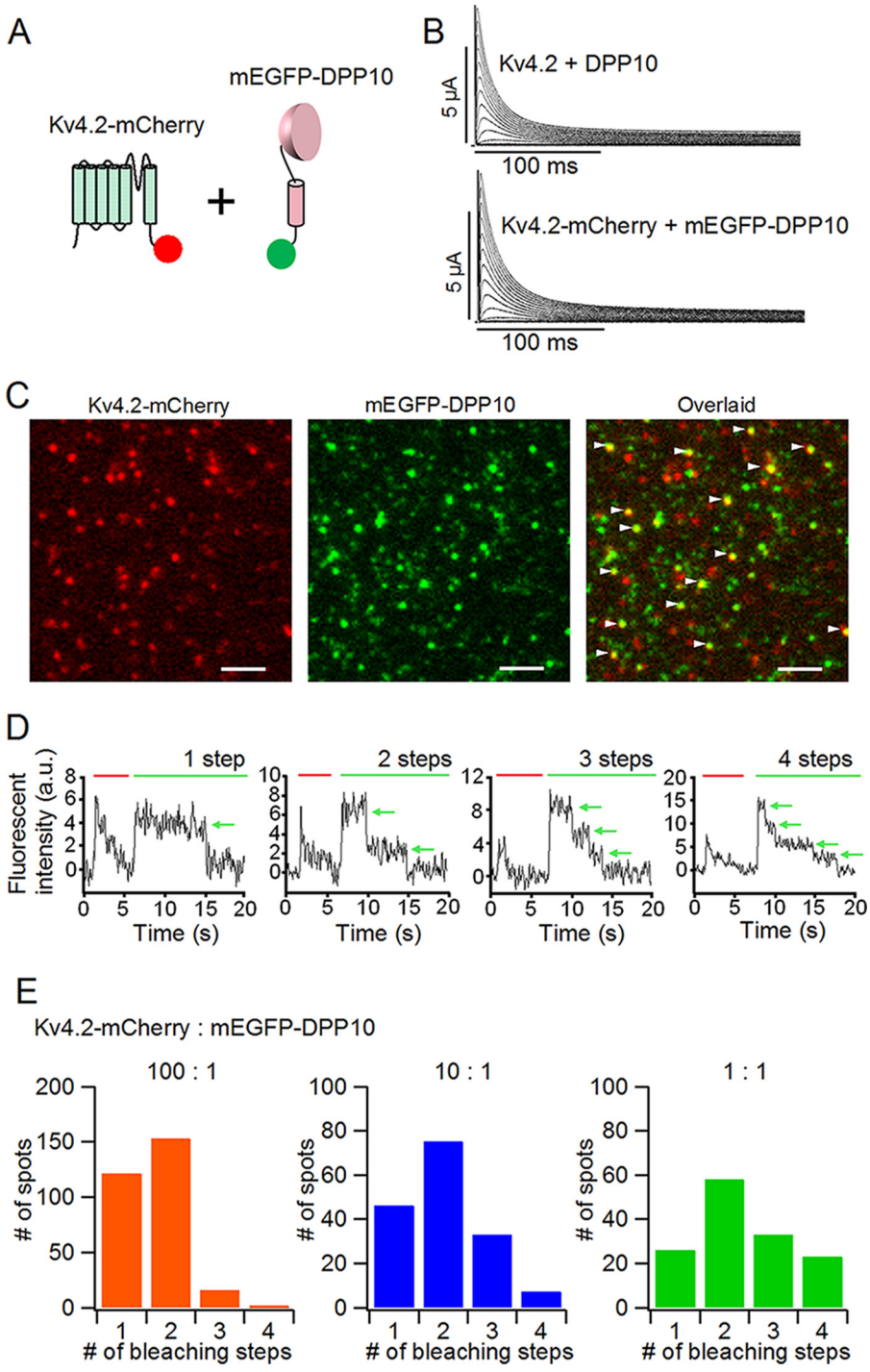

FIGURE 4. **The stoichiometry of the Kv4.2-DPP10 complex has a preference of 4:2.** *A*, schematic illustrations of Kv4.2-mCherry and mEGFP-DPP10. mCherry is fused to the C terminus of Kv4.2, and mEGFP is fused to the N terminus of DPP10. *B*, representative current traces of Kv4.2 (2.5 ng) with DPP10 (2.5 ng) (*top*) and Kv4.2-mCherry (2.5 ng) with mEGFP-DPP10 (2.5 ng) (*bottom*). *C*, images of fluorescent spots of Kv4.2-mCherry (*left*) and mEGFP-DPP10 (middle) plus overlaid image (*right*). The *white arrowheads* indicate co-localization of Kv4.2-mCherry and mEGFP-DPP10. *Scale bars* = 2 μm. *D*, representative fluorescence traces of one, two, three, and four bleaching steps. The *red bars* indicate illumination with a 588-nm laser, and *green bars* indicate illumination with a 488-nm laser. The *green arrows* show the bleaching steps. *E*, histograms of the distributions of the number of bleaching steps. Kv4.2-mCherry and mEGFP-DPP10 are expressed at different ratios (Kv4.2-mCherry:mEGFP-DPP10 = 100:1, 10:1, and 1:1).

the current amplitude augmentation required relatively high (2.5 ng) DPP10 cRNA (Fig. 1), whereas the recovery from inactivation (Fig. 2) was affected by a much lower amount of DPP10 cRNA. These findings raise the possibility that the number of DPP10 subunits required for each type of modulation is different, *i.e.* a smaller number of DPP10 subunits can accelerate the recovery from inactivation, whereas more subunits are required for the augmentation of the current amplitude.

We observed that Kv4.2 tends to form a 4:2 (Kv4.2:DPP10) complex with DPP10, but additional DPP10 subunits can bind to the 4:2 channel when the DPP10 co-expression is high (Fig. 4). According to a previous study using the tandem repeat con-

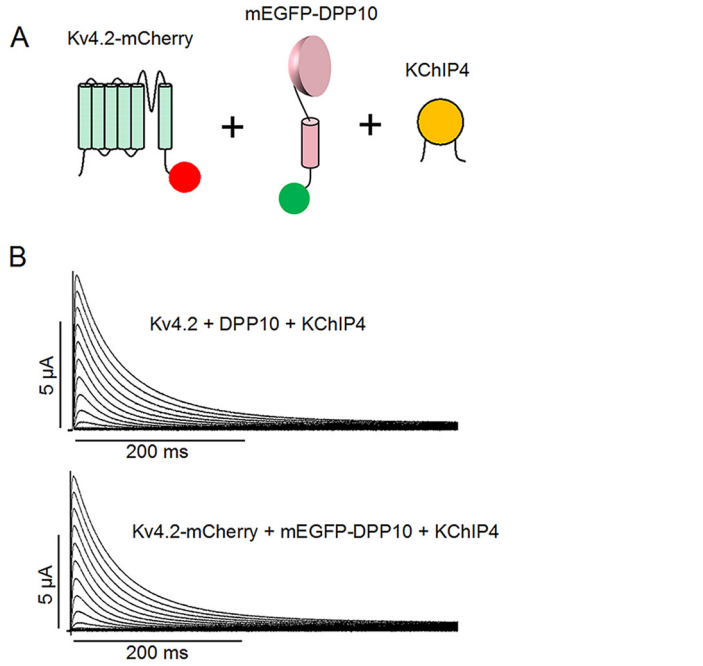

FIGURE 5. **Co-expression of KChIP4 does not affect the stoichiometry of the Kv4.2-DPP10 complex.** *A*, schematic illustrations of Kv4.2-mCherry, mEGFP-DPP10, and KChIP4. *B*, representative current traces of wild-type Kv4.2, wild-type DPP10, and wild-type KChIP4 (*top*) and of Kv4.2-mCherry, mEGFP-DPP10, and wild-type KChIP4 (*bottom*). *C*, Kv4.2-mCherry, KChIP4, and mEGFP-DPP10 were expressed in *Xenopus* oocytes at different ratios (Kv4.2-mCherry:mEGFP-DPP10:KChIP4 = 100:1:100, 10:1:10, and 1:1:1). The histograms show the distributions of the bleaching steps from the spots of mEGFP-DPP10.

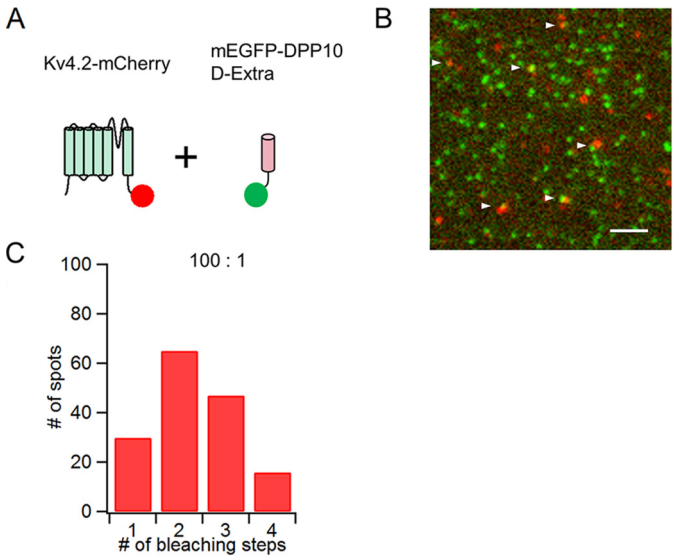

FIGURE 6. **The extracellular domain deletion DPP10 mutant shows less preference for the 4:2 stoichiometry.** *A*, schematic illustrations of Kv4.2-mCherry and mEGFP-DPP10-D-Extra. *B*, image of fluorescent spots of Kv4.2-mCherry (*red*) and mEGFP-DPP10-D-Extra (*green*). The *white arrowheads* indicate co-localization of Kv4.2-mCherry and mEGFP-DPP10-D-Extra. *Scale bar* = 2 μm. *C*, histogram of the distributions of the number of bleaching steps from oocytes expressing Kv4.2-mCherry and mEGFP-DPP10-D-Extra with a 100:1 cRNA ratio.

structs KD (Kv4.2-DPP6) and KKD (Kv4.2-Kv4.2-DPP6), the KKD (4:2) channel can be modulated further by additional DPP6 while the KD (4:4) channel cannot (49). There are a few other notable findings from the previous results: 1) the current amplitude of KD is much higher than that of KKD, suggesting that high DPP expression is required to increase the current amplitude, as we showed in Fig. 1; and 2) the conductance-voltage relationship, the steady state inactivation-voltage relationship, and time to peak are gradually changed from "K" (Kv4.2 alone), through KKD to KD, suggesting that the stoichiometry and function of Kv4.2-DPP6 are variable, as discussed here. Although the conclusion of the authors of the previous study is that Kv4.2 requires four DPP6 subunits to generate I_{SA} current (49), their data also support the idea that the stoichiometry of Kv4.2-DPP is variable.

A Model for Kv4.2-DPP10 Complex Formation—Under the TIRF microscope, we observed that ~70% of the DPP proteins on the membrane exist as dimers and the rest exist as monomers (Fig. 3). This led us to question which form of DPP10 binds to Kv4.2 and forms the complex.

In the previous study using chimeras of Kv4.3/Kv1.4 and DPP10-DPP4, the region from the cytoplasmic N terminus and the transmembrane domain of DPP10 and the S1-S2 segments of Kv4.3 were shown to be sufficient for complex formation (47). It has also been reported that the extracellular domain-less DPP6 mutants (DPP6-D-Extra) can bind to and modulate Kv4.2 channels (41). On the other hand, the crystal structure demonstrates that the extracellular domain of DPP6/10 forms a dimeric structure (26, 48). DPP4, which is a membrane-bound enzyme and does not modulate Kv4, shows catalytic activity when it forms a dimer (63). If the transmembrane domain of DPP binds to the S1 and S2 segments of Kv4, there would be four binding sites for DPPs in one Kv4 channel (Fig. 7*A*). If two DPP10 subunits bind diagonally to Kv4.2, retaining a dimer structure, the dimeric large extracellular domain may hinder the additional binding of a second DPP10 dimer (Fig. 7*Ba*). On the other hand, if the DPP10 dimer can bind to Kv4.2 via one of the transmembrane domains of the dimer, up to eight DPP10 subunits could exist in one Kv4.2-DPP10 complex (Fig. 7*Bb*), although our subunit counting experiments demonstrated that up to four, but no more, DPP10 subunits can bind to a single Kv4.2 channel (Fig. 4). Another possible model of binding is that a DPP10 dimer binds to two neighboring S1-S2 segments (Fig. 7*Bc*). However, this model does not explain why the 4:2 stoichiometry is favored.

How then is the Kv4.2-DPP10 complex formed? Because DPPs can be exported to the plasma membrane without Kv4 and exist as a mixture of monomers and dimers (Fig. 3), one possibility is that the monomeric DPP10 subunits bind to Kv4 and form a dimer in the extracellular domain (Fig. 7*C*). On the

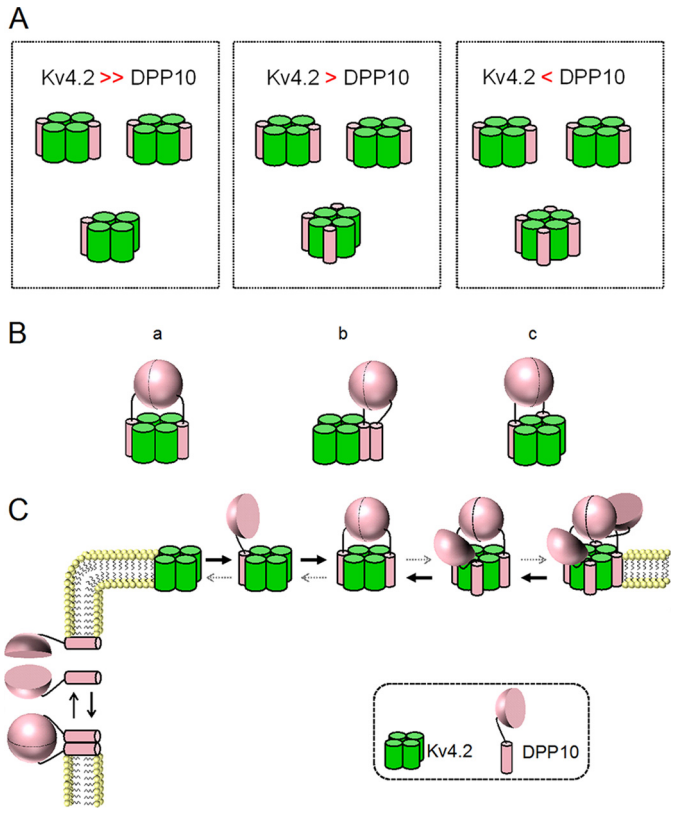

FIGURE 7. **Hypothetical models of Kv4.2-DPP10 complex formation.** *A*, the stoichiometry of the Kv4.2-DPP10 complex changes depending on the relative expression level of Kv4.2 and DPP10 subunits with a preference for 4:2. The *green columns* indicate Kv4.2 α-subunits, and the *pink columns* indicate the transmembrane domain of DPP10. *B*, possible models of the 4:2 (Kv4.2:DPP10) channel complex. *a*, two DPP10 subunits bind to Kv4.2 at diagonal positions. The extracellular domains of two DPP10 subunits bind to each other and prevent an additional DPP10 subunit from binding to Kv4.2. *b*, A DPP10 dimer binds to a single subunit of the Kv4.2 channel. As a tetrameric Kv4.2 channel has four binding sites for DPP10, up to eight DPP10 subunits can bind to one Kv4.2 channel in this configuration, although only a single DPP10 dimer is depicted. *c*, Two DPP10 subunits bind to adjacent binding sites on Kv4.2. The third and fourth DPP10 subunits may be able to bind to Kv4.2 in this configuration. *C*, schematic illustrations of the DPP10 monomer-dimer transition and the Kv4.2-DPP10 complex formation in the plasma membrane. All five stoichiometries (4:0, 4:1, 4:2, 4:3, and 4:4) of the Kv4.2-DPP10 complex are depicted, although the 4:2 stoichiometry is stable because of the dimeric nature of DPP10.

other hand, the dimeric nature of DPP10 may prevent the third and fourth DPP10 subunits from binding to the 4:2 channels. The fact that the extracellular deletion mutant DPP10-D-Extra showed a higher number of three- and four-step bleaching spots supports the idea of a role for the extracellular domain in determining the stoichiometry (Fig. 6).

Is the Stoichiometry of the Kv4-KChIP-DPP Ternary Complex Variable under Physiological Conditions?—It is known that Kv4 forms a ternary complex with DPP and KChIP in the brain (17, 35, 60, 64). In a previous study, we revealed that the stoichiometry of the Kv4.2-KChIP4 complex is variable, with no specific preference, and changes depending on the expression level of KChIP (50). We also showed that the co-expression of DPP10 does not affect the stoichiometry of the Kv4.2-KChIP4 complex (50). In the current study, we also observed that co-expression of KChIP4 does not affect the stoichiometry of the Kv4.2-DPP10 complex. These findings suggest that KChIP and DPP bind independently of each other.

Are the expression levels and the stoichiometry of Kv4-DPP variable? In the case of KChIP2, the expression level is changed dynamically with the circadian rhythm, which could change the stoichiometry of Kv4.2/KChIP2 (65). It is unknown whether the expression level of DPP is controlled dynamically. Interestingly, the graded expression of A-type current (Kv4 current) critically controlled by DPP6 (29) suggests that the subcellular localization of DPP6 might also be graded. DPP6 is basically well co-localized with Kv4.2 in the hippocampus and the cerebellar cortex. DPP6 is also expressed in the hippocampal mossy fibers where Kv4.2 is absent (22) suggesting that the expression of Kv4.2 and DPP6 do not always overlap. DPP10 is also widely co-expressed in many brain regions with Kv4.2 and/or Kv4.3 (35). Interestingly, the sublocalization of DPP10 does not perfectly overlap with Kv4 and KChIP. DPP10 is expressed mainly in the soma, whereas Kv4.3 and KChIP1 are expressed both in the soma and the dendrites of the hippocampus and the neocortex (35). This means that the stoichiometry of the ternary complex may be different depending on the subcellular location.

The expression pattern of DPP10 partially overlaps the distribution pattern of DPP6 (20, 60). Because the amino acid identity of the transmembrane domain between DPP6 and DPP10 is high (91%) and the transmembrane domain of DPP10 is important for the binding to Kv4.2, DPP6 may form a hetero-multimeric complex with DPP10 (47, 48). The combination of Kv4, KChIP, and DPP6/10 in the complex would give rise to further diversity of the biophysical properties and may dynamically regulate cell excitability by a complicated stoichiometry.

Author Contributions—Y. K. and K. N. designed the research. M. K. performed all of the experiments. M. K. and K. N. analyzed the data. All of the authors reviewed the results, wrote the manuscript, and approved the final version of the manuscript.

Acknowledgments—We thank M. Ulbrich (University of Freiburg) for providing the analysis software for subunit counting and the vectors for constructing the mEGFP/mCherry fusion proteins. We thank A. Collins (Queen's University, Belfast) for editing of the English.

References

1. Serôdio, P., Kentros, C., and Rudy, B. (1994) Identification of molecular components of A-type channels activating at subthreshold potentials. *J. Neurophysiol.* **72,** 1516–1529
2. Serôdio, P., Vega-Saenz de Miera, E., and Rudy, B. (1996) Cloning of a novel component of A-type K^+ channels operating at subthreshold potentials with unique expression in heart and brain. *J. Neurophysiol.* **75,** 2174–2179
3. Serodio, P., and Rudy, B. (1998) Differential expression of Kv4 K^+ channel subunits mediating subthreshold transient K^+ (A-type) currents in rat brain. *J. Neurophysiol.* **79,** 1081–1091
4. Rhodes, K. J., Carroll, K. I., Sung, M. A., Doliveira, L. C., Monaghan, M. M., Burke, S. L., Strassle, B. W., Buchwalder, L., Menegola, M., Cao, J., An, W. F., and Trimmer, J. S. (2004) KChIPs and Kv4 α subunits as integral components of A-type potassium channels in mammalian brain. *J. Neurosci.* **24,** 7903–7915
5. Chen, X., Yuan, L. L., Zhao, C., Birnbaum, S. G., Frick, A., Jung, W. E., Schwarz, T. L., Sweatt, J. D., and Johnston, D. (2006) Deletion of Kv4.2 gene eliminates dendritic A-type K^+ current and enhances induction of long-term potentiation in hippocampal CA1 pyramidal neurons. *J. Neurosci.* **26,** 12143–12151

6. Dixon, J. E., and McKinnon, D. (1994) Quantitative analysis of potassium channel mRNA expression in atrial and ventricular muscle of rats. *Circ. Res.* **75,** 252–260
7. Dixon, J. E., Shi, W., Wang, H. S., McDonald, C., Yu, H., Wymore, R. S., Cohen, I. S., and McKinnon, D. (1996) Role of the Kv4.3 K^+ channel in ventricular muscle. A molecular correlate for the transient outward current. *Circ. Res.* **79,** 659–668
8. Brahmajothi, M. V., Campbell, D. L., Rasmusson, R. L., Morales, M. J., Trimmer, J. S., Nerbonne, J. M., and Strauss, H. C. (1999) Distinct transient outward potassium current (I_{to}) phenotypes and distribution of fast-inactivating potassium channel α subunits in ferret left ventricular myocytes. *J. Gen. Physiol.* **113,** 581–600
9. Xu, H., Li, H., and Nerbonne, J. M. (1999) Elimination of the transient outward current and action potential prolongation in mouse atrial myocytes expressing a dominant negative Kv4 α subunit. *J. Physiol.* **519,** 11–21
10. Nerbonne, J. M. (2000) Molecular basis of functional voltage-gated K^+ channel diversity in the mammalian myocardium. *J. Physiol.* **525,** 285–298
11. Deschênes, I., and Tomaselli, G. F. (2002) Modulation of Kv4.3 current by accessory subunits. *FEBS Lett.* **528,** 183–188
12. Sanguinetti, M. C. (2002) Reduced transient outward K^+ current and cardiac hypertrophy: causal relationship or epiphenomenon? *Circ. Res.* **90,** 497–499
13. Nerbonne, J. M., and Kass, R. S. (2005) Molecular physiology of cardiac repolarization. *Physiol. Rev.* **85,** 1205–1253
14. Niwa, N., and Nerbonne, J. M. (2010) Molecular determinants of cardiac transient outward potassium current (I_{to}) expression and regulation. *J. Mol. Cell Cardiol.* **48,** 12–25
15. Birnbaum, S. G., Varga, A. W., Yuan, L. L., Anderson, A. E., Sweatt, J. D., and Schrader, L. A. (2004) Structure and function of Kv4-family transient potassium channels. *Physiol. Rev.* **84,** 803–833
16. Jerng, H. H., and Pfaffinger, P. J. (2008) Multiple Kv channel-interacting proteins contain an N-terminal transmembrane domain that regulates Kv4 channel trafficking and gating. *J. Biol. Chem.* **283,** 36046–36059
17. Jerng, H. H., Pfaffinger, P. J., and Covarrubias, M. (2004) Molecular physiology and modulation of somatodendritic A-type potassium channels. *Mol. Cell. Neurosci.* **27,** 343–369
18. Maffie, J., and Rudy, B. (2008) Weighing the evidence for a ternary protein complex mediating A-type K^+ currents in neurons. *J. Physiol.* **586,** 5609–5623
19. Marionneau, C., Townsend, R. R., and Nerbonne, J. M. (2011) Proteomic analysis highlights the molecular complexities of native Kv4 channel macromolecular complexes. *Semin. Cell Dev. Biol.* **22,** 145–152
20. Pongs, O., and Schwarz, J. R. (2010) Ancillary subunits associated with voltage-dependent K^+ channels. *Physiol. Rev.* **90,** 755–796
21. Nadal, M. S., Ozaita, A., Amarillo, Y., Vega-Saenz de Miera, E., Ma, Y., Mo, W., Goldberg, E. M., Misumi, Y., Ikehara, Y., Neubert, T. A., and Rudy, B. (2003) The CD26-related dipeptidyl aminopeptidase-like protein DPPX is a critical component of neuronal A-type K^+ channels. *Neuron* **37,** 449–461
22. Clark, B. D., Kwon, E., Maffie, J., Jeong, H. Y., Nadal, M., Strop, P., and Rudy, B. (2008) DPP6 Localization in brain supports function as a Kv4 channel-associated protein. *Front. Mol. Neurosci.* **1,** 8
23. Dougherty, K., Tu, L., Deutsch, C., and Covarrubias, M. (2009) The dipeptidyl-aminopeptidase-like protein 6 is an integral voltage sensor-interacting β-subunit of neuronal $K_V4.2$ channels. *Channels* (*Austin*) **3,** 122–128
24. Nadin, B. M., and Pfaffinger, P. J. (2010) Dipeptidyl peptidase-like protein 6 is required for normal electrophysiological properties of cerebellar granule cells. *J. Neurosci.* **30,** 8551–8565
25. Qi, S. Y., Riviere, P. J., Trojnar, J., Junien, J. L., and Akinsanya, K. O. (2003) Cloning and characterization of dipeptidyl peptidase 10, a new member of an emerging subgroup of serine proteases. *Biochem. J.* **373,** 179–189
26. Strop, P., Bankovich, A. J., Hansen, K. C., Garcia, K. C., and Brunger, A. T. (2004) Structure of a human A-type potassium channel interacting protein DPPX, a member of the dipeptidyl aminopeptidase family. *J. Mol. Biol.* **343,** 1055–1065
27. Jerng, H. H., and Pfaffinger, P. J. (2014) Modulatory mechanisms and multiple functions of somatodendritic A-type K^+ channel auxiliary subunits. *Front. Cell. Neurosci.* **8,** 82
28. Lin, L., Sun, W., Throesch, B., Kung, F., Decoster, J. T., Berner, C. J., Cheney, R. E., Rudy, B., and Hoffman, D. A. (2013) DPP6 regulation of dendritic morphogenesis impacts hippocampal synaptic development. *Nat. Commun.* **4,** 2270
29. Sun, W., Maffie, J. K., Lin, L., Petralia, R. S., Rudy, B., and Hoffman, D. A. (2011) DPP6 establishes the A-type K^+ current gradient critical for the regulation of dendritic excitability in CA1 hippocampal neurons. *Neuron* **71,** 1102–1115
30. Marshall, C. R., Noor, A., Vincent, J. B., Lionel, A. C., Feuk, L., Skaug, J., Shago, M., Moessner, R., Pinto, D., Ren, Y., Thiruvahindrapduram, B., Fiebig, A., Schreiber, S., Friedman, J., Ketelaars, C. E., Vos, Y. J., Ficicioglu, C., Kirkpatrick, S., Nicolson, R., Sloman, L., Summers, A., Gibbons, C. A., Teebi, A., Chitayat, D., Weksberg, R., Thompson, A., Vardy, C., Crosbie, V., Luscombe, S., Baatjes, R., Zwaigenbaum, L., Roberts, W., Fernandez, B., Szatmari, P., and Scherer, S. W. (2008) Structural variation of chromosomes in autism spectrum disorder. *Am. J. Hum. Genet.* **82,** 477–488
31. Noor, A., Whibley, A., Marshall, C. R., Gianakopoulos, P. J., Piton, A., Carson, A. R., Orlic-Milacic, M., Lionel, A. C., Sato, D., Pinto, D., Drmic, I., Noakes, C., Senman, L., Zhang, X., Mo, R., Gauthier, J., Crosbie, J., Pagnamenta, A. T., Munson, J., Estes, A. M., Fiebig, A., Franke, A., Schreiber, S., Stewart, A. F., Roberts, R., McPherson, R., Guter, S. J., Cook, E. H., Jr., Dawson, G., Schellenberg, G. D., Battaglia, A., Maestrini, E., Autism Genome Project Consortium, C., Jeng, L., Hutchison, T., Rajcan-Separovic, E., Chudley, A. E., Lewis, S. M., Liu, X., Holden, J. J., Fernandez, B., Zwaigenbaum, L., Bryson, S. E., Roberts, W., Szatmari, P., Gallagher, L., Stratton, M. R., Gecz, J., Brady, A. F., Schwartz, C. E., Schachar, R. J., Monaco, A. P., Rouleau, G. A., Hui, C. C., Lucy Raymond, F., Scherer, S. W., and Vincent, J. B. (2010) Disruption at the *PTCHD1* locus on Xp22.11 in autism spectrum disorder and intellectual disability. *Sci. Transl. Med.* **2,** 49ra68
32. Liao, C., Fu, F., Li, R., Yang, W. Q., Liao, H. Y., Yan, J. R., Li, J., Li, S. Y., Yang, X., and Li, D. Z. (2013) Loss-of-function variation in the DPP6 gene is associated with autosomal dominant microcephaly and mental retardation. *Eur. J. Med. Genet.* **56,** 484–489
33. Cronin, S., Berger, S., Ding, J., Schymick, J. C., Washecka, N., Hernandez, D. G., Greenway, M. J., Bradley, D. G., Traynor, B. J., and Hardiman, O. (2008) A genome-wide association study of sporadic ALS in a homogenous Irish population. *Hum. Mol. Genet.* **17,** 768–774
34. van Es, M. A., van Vught, P. W., Blauw, H. M., Franke, L., Saris, C. G., Van den Bosch, L., de Jong, S. W., de Jong, V., Baas, F., van't Slot, R., Lemmens, R., Schelhaas, H. J., Birve, A., Sleegers, K., Van Broeckhoven, C., Schymick, J. C., Traynor, B. J., Wokke, J. H., Wijmenga, C., Robberecht, W., Andersen, P. M., Veldink, J. H., Ophoff, R. A., and van den Berg, L. H. (2008) Genetic variation in DPP6 is associated with susceptibility to amyotrophic lateral sclerosis. *Nat. Genet.* **40,** 29–31
35. Wang, W. C., Cheng, C. F., and Tsaur, M. L. (2015) Immunohistochemical localization of DPP10 in rat brain supports the existence of a Kv4/KChIP/DPPL ternary complex in neurons. *J. Comp. Neurol.* **523,** 608–628
36. Girirajan, S., Dennis, M. Y., Baker, C., Malig, M., Coe, B. P., Campbell, C. D., Mark, K., Vu, T. H., Alkan, C., Cheng, Z., Biesecker, L. G., Bernier, R., and Eichler, E. E. (2013) Refinement and discovery of new hotspots of copy-number variation associated with autism spectrum disorder. *Am. J. Hum. Genet.* **92,** 221–237
37. Chen, T., Gai, W. P., and Abbott, C. A. (2014) Dipeptidyl peptidase 10 (DPP10(789)): a voltage-gated potassium channel-associated protein is abnormally expressed in Alzheimer's and other neurodegenerative diseases. *BioMed Res. Int.* **2014,** 209398
38. Zagha, E., Ozaita, A., Chang, S. Y., Nadal, M. S., Lin, U., Saganich, M. J., McCormack, T., Akinsanya, K. O., Qi, S. Y., and Rudy, B. (2005) DPP10 modulates Kv4-mediated A-type potassium channels. *J. Biol. Chem.* **280,** 18853–18861
39. Kaulin, Y. A., De Santiago-Castillo, J. A., Rocha, C. A., Nadal, M. S., Rudy, B., and Covarrubias, M. (2009) The dipeptidyl-peptidase-like protein DPP6 determines the unitary conductance of neuronal Kv4.2 channels. *J. Neurosci.* **29,** 3242–3251
40. Seikel, E., and Trimmer, J. S. (2009) Convergent modulation of Kv4.2 channel α subunits by structurally distinct DPPX and KChIP auxiliary subunits. *Biochemistry* **48,** 5721–5730

41. Lin, L., Long, L. K., Hatch, M. M., and Hoffman, D. A. (2014) DPP6 domains responsible for its localization and function. *J. Biol. Chem.* **289,** 32153–32165
42. Jerng, H. H., Qian, Y., and Pfaffinger, P. J. (2004) Modulation of Kv4.2 channel expression and gating by dipeptidyl peptidase 10 (DPP10). *Biophys. J.* **87,** 2380–2396
43. Radicke, S., Cotella, D., Graf, E. M., Ravens, U., and Wettwer, E. (2005) Expression and function of dipeptidyl-aminopeptidase-like protein 6 as a putative β-subunit of human cardiac transient outward current encoded by Kv4.3. *J. Physiol.* **565,** 751–756
44. Takimoto, K., Hayashi, Y., Ren, X., and Yoshimura, N. (2006) Species and tissue differences in the expression of DPPY splicing variants. *Biochem. Biophys. Res. Commun.* **348,** 1094–1100
45. Jerng, H. H., Lauver, A. D., and Pfaffinger, P. J. (2007) DPP10 splice variants are localized in distinct neuronal populations and act to differentially regulate the inactivation properties of Kv4-based ion channels. *Mol. Cell. Neurosci.* **35,** 604–624
46. Jerng, H. H., Dougherty, K., Covarrubias, M., and Pfaffinger, P. J. (2009) A novel N-terminal motif of dipeptidyl peptidase-like proteins produces rapid inactivation of $K_V4.2$ channels by a pore-blocking mechanism. *Channels* (*Austin*) **3,** 448–461
47. Ren, X., Hayashi, Y., Yoshimura, N., and Takimoto, K. (2005) Transmembrane interaction mediates complex formation between peptidase homologues and Kv4 channels. *Mol. Cell. Neurosci.* **29,** 320–332
48. Bezerra, G. A., Dobrovetsky, E., Seitova, A., Fedosyuk, S., Dhe-Paganon, S., and Gruber, K. (2015) Structure of human dipeptidyl peptidase 10 (DPPY): a modulator of neuronal Kv4 channels. *Sci. Rep.* **5,** 8769
49. Soh, H., and Goldstein, S. A. (2008) I SA channel complexes include four subunits each of DPP6 and Kv4.2. *J. Biol. Chem.* **283,** 15072–15077
50. Kitazawa, M., Kubo, Y., and Nakajo, K. (2014) The stoichiometry and biophysical properties of the Kv4 potassium channel complex with K^+ channel-interacting protein (KChIP) subunits are variable, depending on the relative expression level. *J. Biol. Chem.* **289,** 17597–17609
51. Nakajo, K., Ulbrich, M. H., Kubo, Y., and Isacoff, E. Y. (2010) Stoichiometry of the KCNQ1 - KCNE1 ion channel complex. *Proc. Natl. Acad. Sci. U.S.A.* **107,** 18862–18867
52. Ulbrich, M. H., and Isacoff, E. Y. (2007) Subunit counting in membrane-bound proteins. *Nat. Methods* **4,** 319–321
53. Ulbrich, M. H., and Isacoff, E. Y. (2008) Rules of engagement for NMDA receptor subunits. *Proc. Natl. Acad. Sci. U.S.A.* **105,** 14163–14168
54. Nadal, M. S., Amarillo, Y., Vega-Saenz de Miera, E., and Rudy, B. (2006) Differential characterization of three alternative spliced isoforms of DPPX. *Brain Res.* **1094,** 1–12
55. Arant, R. J., and Ulbrich, M. H. (2014) Deciphering the subunit composition of multimeric proteins by counting photobleaching steps. *Chemphyschem* **15,** 600–605
56. Hastie, P., Ulbrich, M. H., Wang, H. L., Arant, R. J., Lau, A. G., Zhang, Z., Isacoff, E. Y., and Chen, L. (2013) AMPA receptor/TARP stoichiometry visualized by single-molecule subunit counting. *Proc. Natl. Acad. Sci. U.S.A.* **110,** 5163–5168
57. Zhou, J., Tang, Y., Zheng, Q., Li, M., Yuan, T., Chen, L., Huang, Z., and Wang, K. (2015) Different KChIPs compete for heteromultimeric assembly with pore-forming Kv4 subunits. *Biophys. J.* **108,** 2658–2669
58. Kim, J., Nadal, M. S., Clemens, A. M., Baron, M., Jung, S. C., Misumi, Y., Rudy, B., and Hoffman, D. A. (2008) Kv4 accessory protein DPPX (DPP6) is a critical regulator of membrane excitability in hippocampal CA1 pyramidal neurons. *J. Neurophysiol.* **100,** 1835–1847
59. Jerng, H. H., and Pfaffinger, P. J. (2012) Incorporation of DPP6a and DPP6K variants in ternary Kv4 channel complex reconstitutes properties of A-type K current in rat cerebellar granule cells. *PLoS One* **7,** e38205
60. Jerng, H. H., Kunjilwar, K., and Pfaffinger, P. J. (2005) Multiprotein assembly of Kv4.2, KChIP3 and DPP10 produces ternary channel complexes with ISA-like properties. *J. Physiol.* **568,** 767–788
61. Amarillo, Y., De Santiago-Castillo, J. A., Dougherty, K., Maffie, J., Kwon, E., Covarrubias, M., and Rudy, B. (2008) Ternary Kv4.2 channels recapitulate voltage-dependent inactivation kinetics of A-type K+ channels in cerebellar granule neurons. *J. Physiol.* **586,** 2093–2106
62. Foeger, N. C., Norris, A. J., Wren, L. M., and Nerbonne, J. M. (2012) Augmentation of Kv4.2-encoded currents by accessory dipeptidyl peptidase 6 and 10 subunits reflects selective cell surface Kv4.2 protein stabilization. *J. Biol. Chem.* **287,** 9640–9650
63. Chien, C. H., Huang, L. H., Chou, C. Y., Chen, Y. S., Han, Y. S., Chang, G. G., Liang, P. H., and Chen, X. (2004) One site mutation disrupts dimer formation in human DPP-IV proteins. *J. Biol. Chem.* **279,** 52338–52345
64. Matsuyoshi, H., Takimoto, K., Yunoki, T., Erickson, V. L., Tyagi, P., Hirao, Y., Wanaka, A., and Yoshimura, N. (2012) Distinct cellular distributions of Kv4 pore-forming and auxiliary subunits in rat dorsal root ganglion neurons. *Life Sci.* **91,** 258–263
65. Jeyaraj, D., Haldar, S. M., Wan, X., McCauley, M. D., Ripperger, J. A., Hu, K., Lu, Y., Eapen, B. L., Sharma, N., Ficker, E., Cutler, M. J., Gulick, J., Sanbe, A., Robbins, J., Demolombe, S., Kondratov, R. V., Shea, S. A., Albrecht, U., Wehrens, X. H., Rosenbaum, D. S., and Jain, M. K. (2012) Circadian rhythms govern cardiac repolarization and arrhythmogenesis. *Nature* **483,** 96–99